

# Electrochemical Preparation of Porous PtCu Alloy on an Ionic Liquid Functionalized Graphene Film for the Electrocatalytic Oxidation and Amperometric Detection of Ethanol

Fang Xu, Lite Yang, Faqiong Zhao, Baizhao Zeng\*

Key Laboratory of Analytical Chemistry for Biology and Medicine (Ministry of Education), College of Chemistry and Molecular Sciences, Wuhan University, Wuhan 430072, Hubei Province, P. R. China

\*E-mail: [bzzeng@whu.edu.cn](mailto:bzzeng@whu.edu.cn)

Received: 29 September 2015 / Accepted: 14 December 2015 / Published: 1 January 2016

---

A novel porous PtCu film was prepared on an ionic liquid functionalized graphene film by electrodeposition and electrochemical oxidation. The porous PtCu film showed the features of alloy and had large active surface area. Its electrocatalytic activity was explored by taking ethanol as a model molecule, which exhibited sensitive oxidation peaks at the resulting electrode in H<sub>2</sub>SO<sub>4</sub> solutions. Under the optimized conditions the oxidation current of ethanol at 0.65 V (vs SCE) was linear to its concentration in the range of 0.25–13 mM, the sensitivity was 11 μA mM<sup>-1</sup>cm<sup>-2</sup> and the detection limit was 0.05 mM (S/N=3). The electrode was successfully applied to the determination of ethanol in alcoholic samples.

---

**Keywords:** PtCu alloy; Graphene; Electrodeposition; Ethanol; Ionic liquid

## 1. INTRODUCTION

Alloys generally show better properties than the corresponding monometallic components [1], such as higher catalytic activity and anti-poisoning ability. Among various alloys platinum-based alloys have attracted more attention of researchers in electrochemistry field because they present high electrocatalytic activity [2-6]. Some platinum alloys are good catalyst for the electrocatalytic oxidation of ethanol [7-9]. As the catalytic efficiency of catalysts also closely depends on their specific surface, platinum alloy catalysts with nanostructure or porous structure are favorable and often developed [10, 11]. For example, Yang et al [10] prepared PtBi nanoparticles for the electrocatalytic oxidation of methanol and they showed high catalytic activity in acidic solutions. Wang et al [11] reported that the PtSn alloy nanoparticles had high catalytic activity and stability for the electrocatalytic oxidation of

alcohol. Ren et al [12] synthesized PtPd alloy catalysts with different Pt/Pd ratios in the absence of any stabilizers or surfactants, and they demonstrated that the PtPd alloy catalysts had high electrocatalytic activity for ethanol oxidation. However, to the best of our knowledge there are no reports about the amperometric determination of ethanol by using a porous PtCu alloy electrode.

Alloy catalysts can be prepared by various methods, among them electrodeposition method is more simple and controllable. For electrodeposition the support is important; it should be conductive and stable and has large specific surface. Graphene is a novel carbon nanomaterial and it presents good physicochemical properties, such as high thermal stability [13], high electronmobility [14] and high specific surface area [15]. Therefore, it should be a good support for electrodeposition. Graphene can be prepared by chemical reduction and electrochemical reduction. Guo et al thought that the graphene prepared by electrochemical reduction had superior electronic property [16-18]. In addition, Liu et al reported that the re-aggregation of graphene nanosheets could be prevented by functionalizing with ionic liquid (IL) [19, 20].

In this work, IL functionalized graphene was prepared by electrochemical reduction, and PtCu alloy was electrodeposited on the IL functionalized graphene. After part of Cu was removed by electrochemical oxidation a novel porous PtCu alloy was obtained. The electrocatalytic activity of the resulting porous alloy was explored by taking ethanol as a model molecule. It showed high electrocatalysis to the oxidation of ethanol. When it was used for the amperometric determination of ethanol it presented the advantages of short response time, high sensitivity and reproducibility.

## 2. EXPERIMENTAL

### 2.1. Reagents

$\text{H}_2\text{PtCl}_6$  and  $\text{CuSO}_4$  were purchased from Sinopharm Chemical Reagent Co. Ltd. (Shanghai, China). The ionic liquid 1-(2-hydroxyethyl)-3-methylimidazolium bis(trifluoromethanesulfonyl)imide (purity: 99%) was provided by Lanzhou Institute of Chemical Physics (Lanzhou, China) and was used as received. Graphene oxide (GO) came from Xianfeng Reagent Co. Ltd. (Nanjing, China). Ethanol was the product of Sinopharm Chemical Reagent Co. Ltd. (Shanghai, China), and 0.5 mM ethanol solutions were prepared with 0.5 M  $\text{H}_2\text{SO}_4$  solutions and were stored in a refrigerator. All other chemicals used were of analytical reagent grade. The water used was redistilled.

### 2.2. Apparatus

Electrodeposition, cyclic voltammetric and chronoamperometric experiments were performed with a CHI 660D electrochemical workstation (CH Instrument Company, Shanghai, China). A conventional three-electrode system was adopted. The working electrode was a modified glassy carbon electrode (GCE, diameter: 2 mm) or an indium tin oxide (ITO) electrode, and the auxiliary and reference electrodes were a platinum wire and a saturated calomel electrode (SCE), respectively. The scanning electron microscope (SEM) image and energy dispersive X-ray spectroscopy (EDS) were

obtained using a Hitachi X-650 SEM (Hitachi Co., Japan). X-ray diffraction (XRD) experiments were performed with a Bruke D8 diffractometer (Germany) using Cu K $\alpha$  radiation (40 kV, 40 mA) with a Ni filter. All experiments were conducted at room temperature.

### 2.3. Preparation of modified layer

Firstly, GO was dispersed in redistilled water to prepare 1 mg/mL suspension, then 1 mL GO suspension and 1 mL IL solution (5  $\mu$ L/mL, in dimethyl formamide (DMF)) were mixed with the aid of ultrasonication. Following this, 4  $\mu$ L of the resulting suspension was transferred on a cleaned GCE (or ITO) and dried in air. Thus, an IL-GO film coated electrode (IL-GO/GCE) was obtained. The GO-IL/GCE was reduced at -1.3 V for 600 s in phosphate buffer solution (pH=6.0) and the resulting electrode was denoted as EGN-IL/GCE. PtCu was electrodeposited on the EGN-IL/GCE from the electrolyte solution of 1 mM H<sub>2</sub>Pt<sub>6</sub>Cl<sub>4</sub> + 100 mM CuSO<sub>4</sub> + 0.2 M Na<sub>2</sub>SO<sub>4</sub>. The electrodeposition potential was -0.2 V and the electrodeposition time was 500 s. The obtained electrode (PtCu/EGN-IL/GCE) was washed carefully with redistilled water. Then it undergone repetitive cyclic potential scan (about 10 circles) between -0.3 V and 1.2 V in a 0.5 M H<sub>2</sub>SO<sub>4</sub> solution until a stable cyclic voltammogram was obtained. Thus part of Cu was removed and a porous PtCu-EGN-IL/GCE was obtained. For comparison, PtCu/GCE and Pt/EGN-IL/GCE were fabricated through the similar method.

### 2.4. Electrochemical measurement

An 8 mL 0.5 M H<sub>2</sub>SO<sub>4</sub> and proper amount of ethanol were transferred to a 10 mL cell, then the electrode system was installed on it. Cyclic voltammograms were recorded between -0.4 V and 1.6 V, and chronoamperometric response curves were recorded at 0.65 V.

## 3. RESULTS AND DISCUSSION

### 3.1. Morphological analysis

Fig.1 shows the SEM images of different film. As can be seen, EGN presents the typical wrinkled sheet structure of graphene [21]. However, EGN-IL film is quite smooth due to the blanketing effect of viscous IL. Furthermore, the EGN-IL film is more stable than the EGN film on ITO (or GCE). After PtCu is electrodeposited on the EGN-IL film a lot of particles (diameter : about 2  $\mu$ m) occur, which are smaller than those electrodeposited on ITO. The reason is that the EGN-IL film has larger active surface and can provide more sites for the formation of PtCu nucleus. After the PtCu-EGN-IL/GCE is pretreated by cycling the potential between -0.3 V and 1.2 V part of Cu is removed and porous PtCu is obtained. Hence, the surface area of the electrode increases greatly. The diameters of the pores are about 2  $\mu$ m and the wall thickness is about 100 nm.

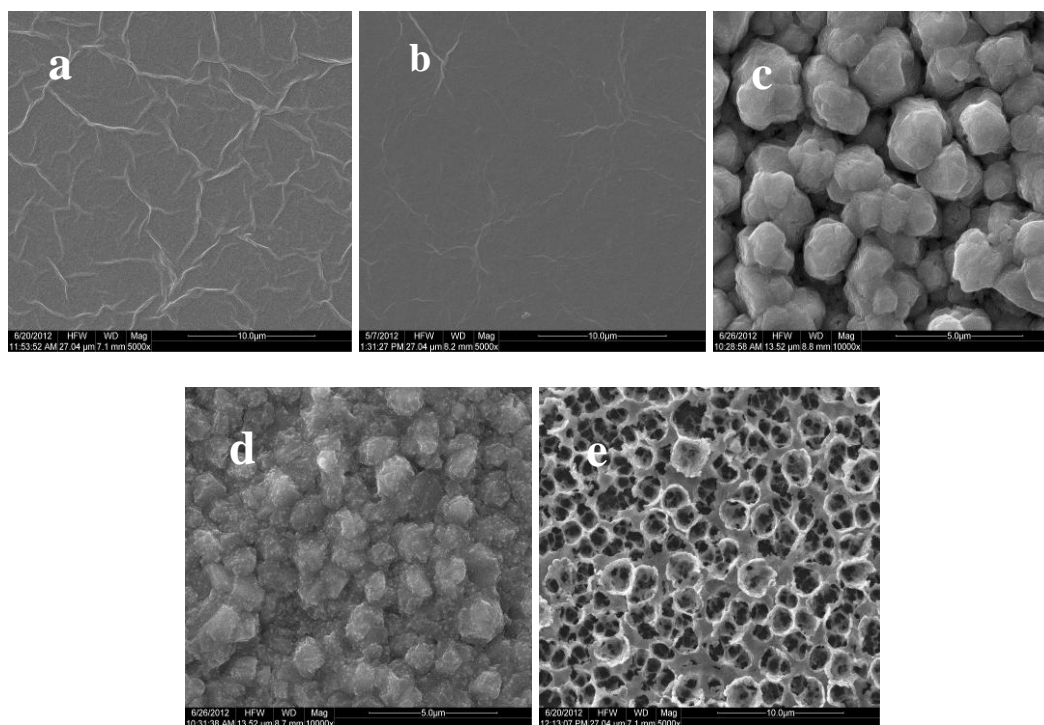


**Figure 1.** SEM images of EGN (a), EGN-IL/ITO (b), PtCu/ITO(c) , PtCu-EGN-IL/ITO (d) and porous PtCu-EGN-IL/ITO (e). The solution composition (for electrodeposition): 0.2 M  $\text{Na}_2\text{SO}_4$  + 1.0 mM  $\text{H}_2\text{Pt}_6\text{Cl}_4$  + 100 mM  $\text{CuSO}_4$ ; electrodeposition potential: -0.2 V; electrodeposition time: 500 s.

### 3.2. Composition and structure analysis

The composition of porous PtCu film was detected by EDS (see Supporting Materials, Fig. S1). The result showed that the atomic ratio of Pt:Cu was about 1:1, indicating that the porous film contained Cu. We thought that only part of Cu formed alloy with Pt during the electrodeposition and it was more difficult for this part of Cu to oxidize. This point was supported by the cyclic voltammetric experiment as shown in Fig. 2B. When the potential scan was repeated the oxidation peak of Cu (around 0 V) decreased rapidly, and the cyclic voltammogram gradually became stable. As the resulting porous film still contained some Cu, it could be deduced that the Cu in alloy was more stable.

Fig. 2A shows the XRD patterns of Pt, Cu, PtCu and porous PtCu electrodeposited on EGN-IL/ITO. A series of broad Bragg peaks occur, and it is typical for material of limited structural coherence. For the electrodeposited Pt the peaks at  $39.71^\circ$ ,  $46.11^\circ$  and  $67.32^\circ$  can be ascribed to the diffraction of Pt (111), (200) and (220), respectively. They are in accord with the standard XRD pattern of Pt (JCPDS 04-0784). The peaks at  $54^\circ$  and  $60^\circ$  are caused by ITO. Although the XRD signals of porous PtCu are weak due to the small amount remained on the EGN-IL/ITO, it can be seen that the peaks of porous PtCu shift to higher  $2\theta$  values in comparison with the corresponding peaks of Pt and locate between the peaks of pure Pt and Cu (JCPDS 04-0836). This indicates that the porous PtCu is alloy rather than a mixture of monometallic materials. It should be mentioned that the pattern

of PtCu (before removing Cu) is similar to that of Cu in this case. The reason is that the content of Pt in PtCu film is very low.

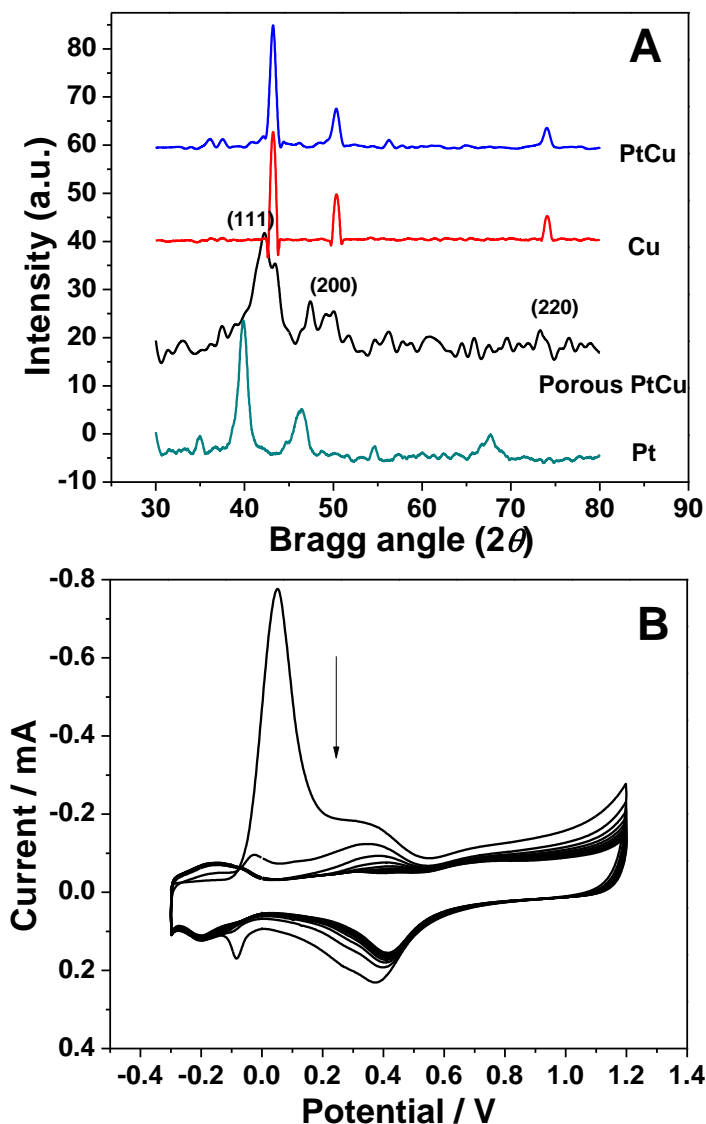


**Figure 2.** (A) XRD patterns of PtCu, Cu, porous PtCu and Pt (from upper to bottom) electrodeposited on EGN-IL film. (B) Cyclic voltammograms of PtCu-EGN-IL/GCE in 0.5 M H<sub>2</sub>SO<sub>4</sub> (from outer to inner: 1<sup>st</sup> CV to 10<sup>th</sup> CV). Scan rate: 100 mV s<sup>-1</sup>.

### 3.3. Electrochemical characterization of PtCu-EGN-IL/GCE

The voltammogram of porous PtCu-EGN-IL/GCE is shown in Fig. 3. As can be seen, in 0.5 M H<sub>2</sub>SO<sub>4</sub> it exhibits a cathodic peak at about 0.4 V, which can be ascribed to the reduction of platinum oxide. The peak of porous PtCu-EGN-IL/GCE is much bigger than that of Pt-EGN-IL/GCE, meaning that in the presence of Cu<sup>2+</sup> more Pt is electrodeposited. According to the equation [22, 23]:  $EASA = Q_H / Q_0$  (where EASA stands for electrochemical active surface area,  $Q_0$  is commonly taken as

$0.21 \text{ mC cm}^{-2}$  and  $Q_H$  is the charge consumed during hydrogen adsorption), the EASAs of porous PtCu-EGN-IL/GCE and Pt-EGN-IL/GCE are estimated and they are  $1.15 \text{ cm}^2$  and  $0.48 \text{ cm}^2$ , respectively. This indicates that the porous PtCu-EGN-IL/GCE has larger Pt surface area.

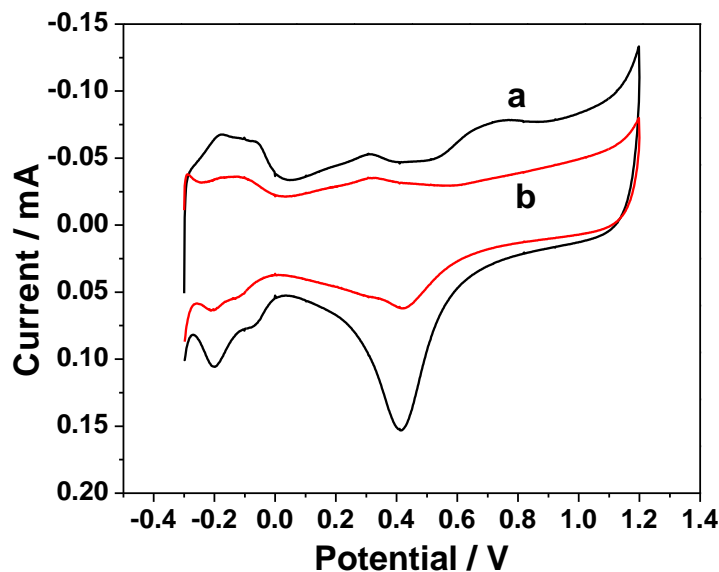


**Figure 3.** Cyclic voltammograms of porous PtCu-EGN-IL/GCE (a) and Pt-EGN-IL/GCE (b) in 0.5 M  $\text{H}_2\text{SO}_4$ . Scan rate:  $100 \text{ mV s}^{-1}$ .

### 3.4. Electrocatalytic oxidation of ethanol

The cyclic voltammograms of ethanol at GCE, EGN-IL/GCE, porous PtCu/GCE, Pt-EGN-IL/GCE, porous PtCu-EGN/GCE and porous PtCu-EGN-IL/GCE are shown in Fig. 4. Ethanol does not produce any peaks at bare GCE and EGN-IL/GCE, but it exhibits peaks at other electrodes. For different electrodes the peak current ( $I_p$ ) follows such order as:  $I_p(\text{porous PtCu/GCE}) < I_p(\text{Pt-EGN-IL/GCE}) < I_p(\text{porous PtCu-EGN/GCE}) < I_p(\text{porous PtCu-EGN-IL/GCE})$ . This means that the porous PtCu-EGN-IL/GCE has larger catalytic surface and/or higher catalytic activity. Part of the reason is that both EGN and IL can promote the electrodeposition of PtCu, and more PtCu is electrodeposited on the EGN-IL film.

As expected the concentrations of  $\text{H}_2\text{PtCl}_6$  and  $\text{CuSO}_4$  affected the peak currents (or oxidation) of ethanol at the resulting porous PtCu-EGN-IL/GCE (Fig. S2 A). When the concentration of  $\text{H}_2\text{PtCl}_6$  was 1 mM, the peak currents of ethanol increased with enhancing  $\text{CuSO}_4$  concentration until it was up to 100 mM. Further increasing  $\text{CuSO}_4$  concentration the peak currents decreased. Therefore, 1 mM  $\text{H}_2\text{PtCl}_6$  and 100 mM  $\text{CuSO}_4$  were used in the following experiments.

Electrodeposition potential also showed some influence on the peak current of ethanol. When it was -0.2 V, the peaks of ethanol were higher. When it was more positive or more negative, the peaks became smaller (Fig S2 B). This was mainly related to the change of alloy amount electrodeposited.

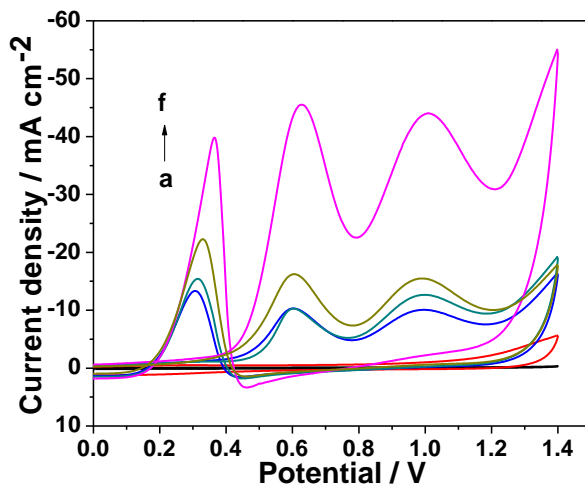


**Figure 4.** Cyclic voltammograms of GCE (a), EGN-IL/GCE(b), porous PtCu/GCE (c), Pt-EGN-IL/GCE (d), porous PtCu-EGN/GCE (e) and porous PtCu-EGN-IL/GCE (f) in 0.5 M H<sub>2</sub>SO<sub>4</sub> containing 0.5 M ethanol.

The influence of electrodeposition time was also explored (Fig S2 C). As a result, when it was increased more PtCu was electrodeposited on the EGN-IL/GCE, and the peaks of ethanol were bigger. The peak currents reached maximum values around 500 s. When electrodeposition time was further increased the peak currents decreased. This should be ascribed to the heavily aggregation of PtCu particles, which affected the removing of Cu and made the active surface area of the resulting porous PtCu-EGN-IL/GCE to decrease.

### 3.5. Variation of oxidation current with ethanol concentration

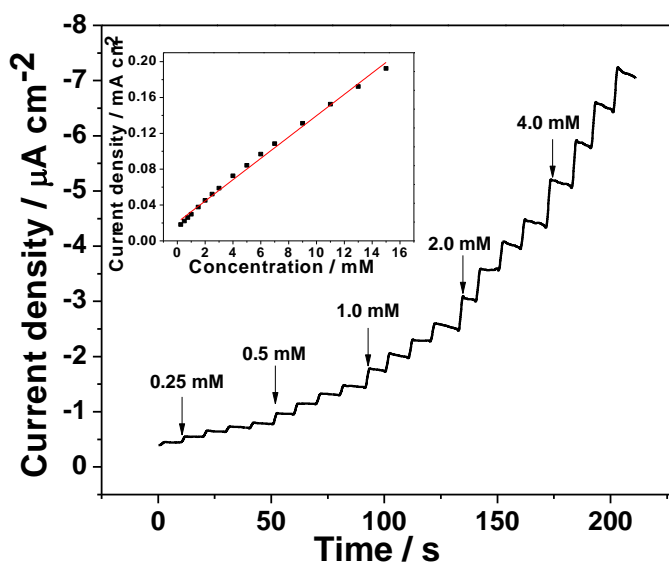


**Figure 5.** Amperometric response of the porous PtCu-EGN-IL/GCE to successive addition of ethanol. Support electrolyte: 0.5 M H<sub>2</sub>SO<sub>4</sub>; applied potential: 0.65 V. Inset: corresponding calibration curve.

The chronoamperometric response curve of the porous PtCu-EGN-IL/GCE to ethanol was recorded (Fig. 5). As could be seen, the oxidation current of ethanol at 0.65 V depended on its concentration. A good linear relationship was obtained over the range of 0.25 –13 mM. The regression equation was  $I \text{ (mA)} = 0.011c + 0.0023$  ( $c$ : mM). The sensitivity was  $11 \mu\text{A mM}^{-1}\text{cm}^{-2}$  and the detection limit was estimated to be 0.05 mM ( $S/N=3$ ). Compared with other electrodes the porous PtCu-EGN-IL/GCE showed good sensitivity and detection limit [24-28] (Table S1).

### 3.6. Stability, reproducibility and interference of foreign species

The reproducibility and stability of the porous PtCu-EGN-IL/GCE were tested. When a 5 mM ethanol solution was measured for 12 times by using a porous PtCu-EGN-IL/GCE the relative standard deviation (RSD) of the response current was 4.5%. When the ethanol solution was measured by using five porous PtCu/EGN-IL/GCE electrodes the RSD was 6.9%. After the porous PtCu-EGN-IL/GCE was stored for one week the current response became 86% of its initial value. After a month-storage it decreased by 26%. This was related to the adsorption of foreign species on porous PtCu-EGN-IL/GCE, which could be reduced by cycling the potential in  $\text{H}_2\text{SO}_4$  solution before measurement.

The influence of some compounds was also tested. The results showed that for 0.5 mM ethanol at least 100-fold glucose, 0.1-fold of methanol and acetaldehyde did not interfere with the determination of ethanol. The influence of ascorbic acid and some easily oxidized substances could be eliminated by measuring the oxidation current at lower potential. Therefore, the porous PtCu-EGN-IL/GCE can be used for the determination of ethanol in some samples.

### 3.7. Application

The proposed method was applied to the determination of ethanol in pineapple beer and white wine (from local market). Prior to determination 200  $\mu\text{L}$  pineapple beer sample was diluted to 10 mL with 0.5 M  $\text{H}_2\text{SO}_4$ , and 10  $\mu\text{L}$  liqueur sample was diluted to 10 mL with 0.5 M  $\text{H}_2\text{SO}_4$ . The measurement results were shown in Table 1. The ethanol contents in the original pineapple beer and liqueur samples were ca. 1.97% and 43.7% respectively, which were in agreement with the declared values on the labels. Standard ethanol solutions were added to the samples to estimate the recoveries and they were 95–102%.

**Table 1.** Measurement results of ethanol in some samples by using the proposed method. (n=5)

Samples	Added (mM)	Found (mM)	RSD (%)	Recovery (%)
Pineapple beer	0.0	6.8	3.8	-
	4.0	10.9±0.2	3.4	102
	8.0	14.9±0.4	4.3	101
Liqueur	0.0	7.5	2.8	-
	4.0	11.3 ± 0.3	2.6	95
	8.0	15.4± 0.3	3.5	99

#### 4. CONCLUSION

In this work, a porous PtCu alloy film was prepared on an ionic liquid functionalized graphene film by electrodeposition and following electrochemical oxidation. The ionic liquid functionalized graphene could promote the deposition of PtCu, and the Cu in PtCu alloy was more difficult to oxide. The resulting porous PtCu alloy film showed large catalytic active surface and platinum was fully used through this way. It exhibited high catalytic activity to the electrocatalytic oxidation of ethanol in H<sub>2</sub>SO<sub>4</sub> solutions. The porous PtCu alloy film had potential application in constructing full cell and ethanol sensor.

#### ACKNOWLEDGEMENTS

The authors appreciate the financial support from the National Natural Science Foundation of China (Grant No.: 21075092 ), the State Key Laboratory of Advanced Technology for Materials Synthesis and Processing (Wuhan University of Technology, Wuhan China, Grant No. 2010-KF-12).

#### References

1. J. J. Huang, W. S. Hwang, Y. C. Weng and T. C. Chou, *Thin Solid Films*, 516 (2008) 5210.
2. M. Chatterjee, A. Chatterjee, S. Ghosh and I. Basumallick, *Electrochim. Acta*, 54 (2009) 7299.
3. J. M. Sieben, M. M. E. Duarte and C. E. Mayer, *J. Appl. Electrochem.*, 38 (2008) 483.
4. C. T. Hsieh, Y. Y. Liu, W. Y. Chen and Y. H. Hsieh, *Int. J. Hydrogen Energy*, 36 (2011) 15766.
5. E. Antolini, F. Colmati and E. R. Gonzalez, *J. Power Sources*, 193 (2009) 555.
6. M. B. de Oliveira, L. P. R. Profeti and P. Olivi, *Electrochem. Commun.*, 7 (2005) 703.
7. B. Liu, H. Y. Li, L. Die, X. H. Zhang, Z. Fan and J. H. Chen, *J. Power Sources*, 186 (2009) 62.
8. E. Devers, C. Geantet, P. Afanasiev, M. Vrinat, M. Aouine and J. L. Zotin, *Appl. Catal. A-Gen.*, 322 (2007) 172.
9. A. Safavi, N. Maleki, F. Farjami and E. Farjami, *J. Electroanal. Chem.*, 626 (2009) 75.
10. M. L. Yang, *J. Power Sources*, 229 (2013) 42.
11. X. Z. Wang, H. Xue, L. J. Yang, H. K. Wang, P. Y. Zang, X. T. Qin, Y. N. Wang, Y. W. Ma, Q. Wu and Z. Hu, *Nanotechnology*, 22 (2011) 395.
12. F. F. Ren, H. W. Wang, C. Y. Zhai, M. S. Zhu, R. R. Yue, Y. K. Du, P. Yang, J. K. Xu and W. S. Lu, *ACS Appl. Mater. Interfaces*, 6 (2014) 3607.
13. A. A. Balandin, S. Ghosh, W. Z. Bao, I. Calizo, D. Teweldebrhan, F. Miao and C. N. Lau, *Nano Lett.*, 8 (2008) 902.
14. R. F. Service, *Science*, 324 (2009) 875.
15. T. N. Lambert, C. A. Chavez, B. Hernandez-Sanchez, P. Lu, N. S. Bell, A. Ambrosini, T. Friedman, T. J. Boyle, D. R. Wheeler and D. L. Huber, *J. Phys. Chem. C*, 113 (2009) 19812.
16. X. H. Wang, I. Kholmanov, H. Chou and R. S. Ruoff, *ACS Nano* 9 (2015) 8737.
17. Y. Y. Shao, J. Wang, M. Engelhard, C. M. Wang and Y. H. Lin, *J. Mater. Chem.*, 20 (2010) 743.
18. S. Wu, X. Q. Lan, L. J. Cui, L. H. Zhang, S. Y. Tao, H. N. Wang, M. Han, Z. G. Liu and C. G. Meng, *Anal. Chim. Acta*, 699 (2011) 170.
19. Z. M. Liu, Z. L. Wang, Y. Y. Cao, Y. F. Jing and Y. L. Liu, *Sens. Actuators B*, 157 (2011) 540.
20. M. H. Yang, B. G. Choi, H. Park, T. J. Park, W. H. Hong and S. Y. Lee, *Electroanalysis*, 23 (2011) 850.
21. L. Y. Chen, Y. H. Tang, K. Wang, C. B. Liu and S. L. Luo, *Electrochem. Commun.*, 13 (2011) 133.
22. M. H. Martin and A. Lasia, *Electrochim. Acta*, 53 (2008) 6317.
23. B. R. Tao, J. Zhang, S. C. Hui and L. J. Wan, *Sens. Actuators B*, 142 (2009) 298.

24. L. N. Wu, M. McIntosh, X. J. Zhang and H. X. Ju, *Talanta* 74 (2007) 387.
25. Y. Liu, L. Zhang, Q. H. Guo, H. Q. Hou and T. Y. You, *Anal. Chim. Acta*, 663 (2010) 153.
26. Y. C. Weng, J. F. Rick and T. C. Chou, *Biosens. Bioelectr.*, 20 (2004) 41.
27. M. M. Barsan and C. M. A. Brett, *Talanta*, 74 (2008) 1505.
28. Y. S. Chen and J. H. Huang, *Biosens. Bioelectr.*, 26 (2010) 207.

© 2016 The Authors. Published by ESG ([www.electrochemsci.org](http://www.electrochemsci.org)). This article is an open access article distributed under the terms and conditions of the Creative Commons Attribution license (<http://creativecommons.org/licenses/by/4.0/>).